

Assessment of Lightning Current Injection Tests in Replicating the In-flight Current Distribution on Aircraft

Surekha Jonnalagadda^{1*}, Udaya Kumar¹

¹ Department of Electrical Engineering, Indian Institute of Science, Bengaluru, India

*E-mail: surekha.j5690@gmail.com

(Received: August 1, 2023, Received in revised form: February 2, 2024, Accepted: February 2, 2024, Available Online)

DOI: <https://doi.org/10.3126/arj.v4i2.65539>

Highlights

- Lightning current distribution on Simple Dynamics Model (SDM) aircraft is evaluated with and without a return conductor (RC) arrangement using the impedance network method.
- It is found that the surface current distribution on aircraft emulated in a laboratory test (with RC) could be different from that experienced in the actual conditions (without RC).
- With the aid of simulation, it is found that in the presence of RC, the current distribution on the wing has been reduced to about 50-60% as compared to that without RC.
- The limitations of the laboratory tests in reproducing the actual current distribution should be considered while designing protective systems for aircraft.
- This work is intended to provide insight into the inherent limitations of laboratory-level testing, which could be helpful for designers.

Abstract

Lightning is one of the natural threats to an aircraft. Laboratory tests are usually limited to aircraft component levels and scaled prototypes. For small aircraft, sometimes the whole aircraft could be subjected to the lightning current specified in the relevant standards. Lightning current injection tests are carried out with standard components A to D. This is in anticipation of producing expected levels of fields and current values during a lightning strike. However, generating a current waveform with a rise time and magnitude the same as component A is very difficult in practice. Further, standards specify a return conductor (RC) arrangement for testing. Fields generated due to RC current can affect the current and field distribution. Hence, the emulated current and field in such tests could differ from that in an actual strike. The present work evaluates the current distribution for different lightning current waveforms suggested in standards and that realised in the laboratory. Also, the effect of the return cage on the current/field distribution is studied. The current and voltage distribution on aircraft skin is obtained by employing the impedance network method. A discretised model of Standard Dynamics Model (SDM) aircraft is employed for the present study. It is found that the surface current distribution on aircraft during a laboratory test can differ from that during the actual strike. Owing to the inductance of the aircraft, the rise time of the lightning current realised in the laboratory could be slow compared to that specified in standards; hence, it could also affect the current distribution on aircraft. This work is intended to provide insight into the inherent limitations of laboratory-level testing, which could be helpful for designers.

Keywords: Aircraft Lightning, High-Current Test, Return Conductor, Impedance Network

*Corresponding author

Introduction

An aircraft could be a potential victim of a lightning strike. There are various documented incidences of aircraft being severely damaged due to the lightning strike [1]–[4]. Field statistics have shown that a typical commercial aircraft is struck by lightning once per year [1], [4]. Probable lightning attachment points are extremities of the aircraft like nose cone, empennage, wings, etc. Lightning stroke currents (ranging from 5 kA to 400 kA) can cause melting/burning/pitting effects, electromagnetic force effects, etc., on metallic aircraft. The fields accompanied during the strike could disrupt/damage the electronic components inside the aircraft. Composite aircraft suffer from resistive heating, shattering of laminates, pyrolysis of resin, etc. Also, the increased use of electronics for flight operations has made aircraft more liable to lightning damage.

Lightning protection schemes are imperative and have to be incorporated during the design stage of aircraft. Lightning Current Injection (LCI) tests are suggested in standards to validate these systems at the laboratory level. These are devised based on the current and field measurements obtained from instrumented aircraft [5]–[8]. The Society of Automotive Engineers (SAE) has published various standard waveforms and testing procedures for lightning certification of aircraft. In SAE-ARP5412, current *component A* is specified for LCI testing with a rise time of 6.4 μs and amplitude of 200 kA [9]. However, it is very difficult to build such a generator. Practical current waveforms generated in the laboratory are much slower compared to that of *component A* due to the loop inductance.

Further, LCI tests are conducted on aircraft with a Return Conductor (RC) arrangement as described in SAE-ARP5416 [10], [11]. RC helps to maintain the rise time of the current waveform the same as that of the actual current. Conducting a laboratory test on aircraft without RC would require a huge generator, which is difficult to construct. For the purpose of testing small aircraft, RC is made of a number of conductors/wires running along the length of the aircraft, encompassing it uniformly at the top and bottom, similar to a coaxial transmission line. The typical structure of RC can be found in [10], [12]. However, during a real lightning strike, the current return path is at infinity. The presence of RC in an LCI test would make the current and field distribution more uniform on the aircraft surface. Hence, the lightning environment emulated in a laboratory test could be different from the actual conditions.

In literature, the effect of return conductors, and their distance from the test body (a metallic cylinder) on the surface current density of the cylinder are analysed by simulation in CST Microwave studio [13], [14]. In our earlier work [11], with the aid of simulation exercises, we have shown that the potential across the aircraft (between injection and ejection points) with and without RC is different and that the potential reduces significantly in the presence of RC.

It can be envisaged that the current density on aircraft surface emulated in a laboratory test could be different from that during the actual lightning strike. The way current distributes on aircraft surface can be explained with the help of a thin conducting plate. For long, thin conducting plate-like structures (thickness is much less than length and width), eddy current effects would lead to a high current density at the edges of the plates, which reduces gradually to a low value at the centre of the plate. This is also termed the lateral skin effect. However, for thin cylindrical shells, eddy currents cancel away, giving a uniform current distribution. In aircraft, this lateral skin effect is more developed in wing regions as they represent thin plates, but in the fuselage region, the current is mostly uniform. Lateral skin depth depends on the frequency of the injected current. Hence, the surface current distribution on aircraft depends on the rise time of the current waveform. For fast-rise times, eddy current effects dominate the current distribution, leading to a high current density at the edges and openings of aircraft and a relatively lower current value at the central body. Because the current waveform generated in the laboratory is much slower compared to the actual current, the surface current distribution is expected to be different from the actual one.

In the present paper, simulation exercises are carried out on a small aircraft model to obtain the current density distribution on aircraft with and without RC. The current distribution is also evaluated for different peak times of injected current waveform, corresponding to the natural environment and that generated in two different high-voltage laboratories in India. In all these cases, the current density on the aircraft surface is computed, and some inferences are made.

Discretised Aircraft Model and Return Conductor Arrangement

A simplified aircraft model for wind tunnel facilities was developed in 1978 by the National Aeronautical Establishment (NAE), Canada, for obtaining experimental static and dynamic aerodynamic derivatives [15]. It is called the Standard Dynamics Model (SDM). It consists of axis-symmetric fuselage/central body, lifting surfaces that are flat and tapered, leading and trailing wing

edges which are chord-wise tapered [15]. Later on, it became a standard model for NASA and AEDC for different wind tunnel testing programs. Subsequently, this model is extensively used by a large number of researchers for acquiring experimental data.

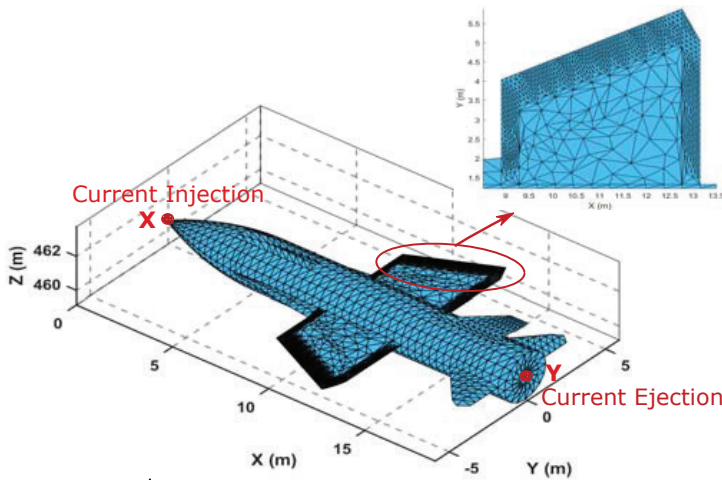


Fig. 1. SDM aircraft model (meshed) with current injection (X) and ejection (Y) points

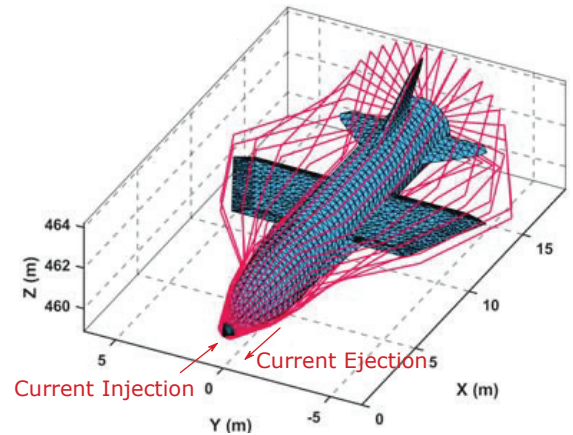


Fig. 2. Return conductor arrangement for the aircraft

This simplified SDM model has been adopted for the present work, as no such standard model is available for experimentation and validation of lightning studies. Fig. 1 shows the SDM discretised model employed. The length of SDM is about 18.8 m and its wing spans about 12 m, and only the outer surface of the aircraft is considered. For numerical analysis, the surface of SDM has been discretised into 9204 triangles/patches which consist of 13882 edges/branches and 4674 nodes. The central body of the aircraft is meshed coarsely; however, in wing regions for an accurate representation of fields, a much finer discretisation is employed. The average discretisation size for this region is taken as 0.05 m. This finer mesh on the wing region is shown in detail with the aid of an arrow in Fig. 1. The return conductor represents a cage-like structure with parallel wires enclosing the aircraft all along its length, and placed at a certain distance from it. The aircraft’s tail end is connected to the RC, and the other end of the RC is grounded. Current, when injected at the nosecone tip, exits at the tail end, and through the return conductor, it passes to the ground. The RC for SDM is shown in Fig. 2, which consists of 32 parallel wires and the spacing between the aircraft surface and RC is about 20-30 cm.

Numerical Methodology

When lightning strikes an aircraft, current passes through the aircraft (skin and air-frame) from one extremity (here referred to as injection point) to another extremity (ejection point) to the ground. Fig. 1 shows the aircraft model, with the current entering at the tip of the aircraft nosecone and leaving at the tail end of the aircraft (conforming with the laboratory tests). Fig. 2 shows the return conductor arrangement built for SDM aircraft, along with the injection and ejection points. In [9], components A to D are defined for carrying out current tests specifically for aircraft. It has been shown in [12] that for the frequencies corresponding to these components, no wave propagation would exist and that the eddy current fields would dominate the current and field distribution on aircraft [12]. Hence, impedance network method is found to be suitable for obtaining the current distribution by representing the geometry of the aircraft as an equivalent network model across injection and ejection points.

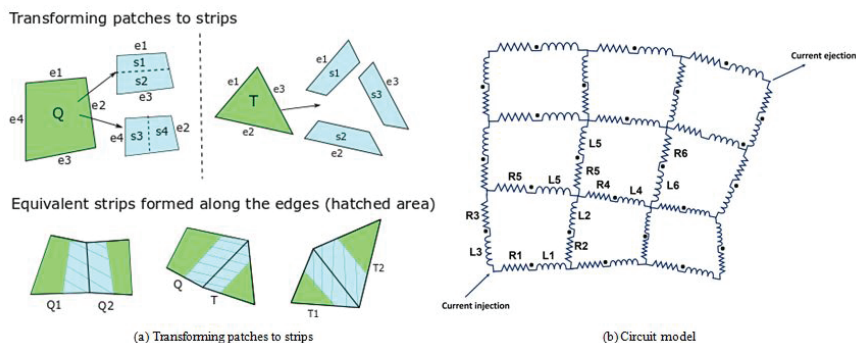


Fig. 3. Impedance network method

Impedance network method is described with the help of Fig. 3. The skin of the aircraft is meshed into quadrilateral (Q1, Q2, ..etc.) or triangular (T1, T2,..etc.) elements, which are also called patches. Each patch (Q/T) is split into strips along the patch edges. As shown in Fig. 3(a), a quadrilateral patch is divided into four strips (S1 to S2) by cutting the patch horizontally as well as vertically parallel to the edges. In Fig. 3(a), strips S1, S2 are associated with edges e1, e3 respectively and strips S3, S4 associated with edges e4, e2 respectively. Similarly, for any triangle, say, T, three strips are formed by cutting it parallel to the edges (Fig. 3(a)). When two adjacent patches meet at a common edge (Q1-Q2, Q-T, T1-T2), they contribute to two strips on both sides of that edge. These two strips are combined to create an equivalent strip representing the shared edge. Fig. 3(a) illustrates the equivalent strips derived from different types of patches, such as quadrilaterals and triangles. Such equivalent strips are formed for all other edges (also called the branches) from patch data. The resulting equivalent strip is attached to the two nodes of the edge. The entire system is then represented as an RL equivalent network model. Fig. 3(b) portrays the resultant RL equivalent network model. In this model, R signifies the strip resistance, and L represents the inductance of the strip. There is mutual coupling among all the strips, indicating interactions or influences between them.

By representing the entire geometry as an impedance network model, a nodal equivalent procedure can be used to find the current and potential distribution on aircraft as well as the RC. The RC wires are discretised into elementary filaments. The analytical formulas given in [16] are utilised to determine the self-inductance of the filaments as well as the strips. Additionally, Neumann's formula (for surface currents) given in equation (1) is applied to assess the mutual inductance of any two strips.

$$M = \frac{\mu_0}{4\pi} \frac{1}{I_s I'_s} \int \int \frac{\vec{J}_s \cdot \vec{J}'_s}{|\vec{r}|} ds' ds \quad (1)$$

where $|\vec{r}|$ = distance between source and measurement point in m , \vec{J}_s = Current density on source surface in A/m , \vec{J}'_s Current density on measurement surface in A/m , I_s = Current on source surface in A , I'_s = Current on measurement surface in A .

Equation (1) is evaluated numerically by Gaussian integration to find the mutual inductance of two strips. Mutual coupling between strip-filament and vice-versa is also computed numerically with the aid of equation (1). Node voltages are assigned to the grids of the meshed geometry. The current that passes between adjacent nodes/grids is called branch current. A code is developed in MATLAB to solve for the unknowns (node voltages and branch currents in the frequency domain) of the equivalent wire mesh network obtained from aircraft and return conductors (for a given injected current). By using the inverse Fourier transform, time domain results are acquired.

The average current density for a specific branch is determined by dividing the branch current by the total width. This total width is the sum of all strip widths connected to the respective branch. Once these average current densities are calculated, plots of current density on patches are generated. This is achieved by summing up the average current densities of all branches linked a particular patch.

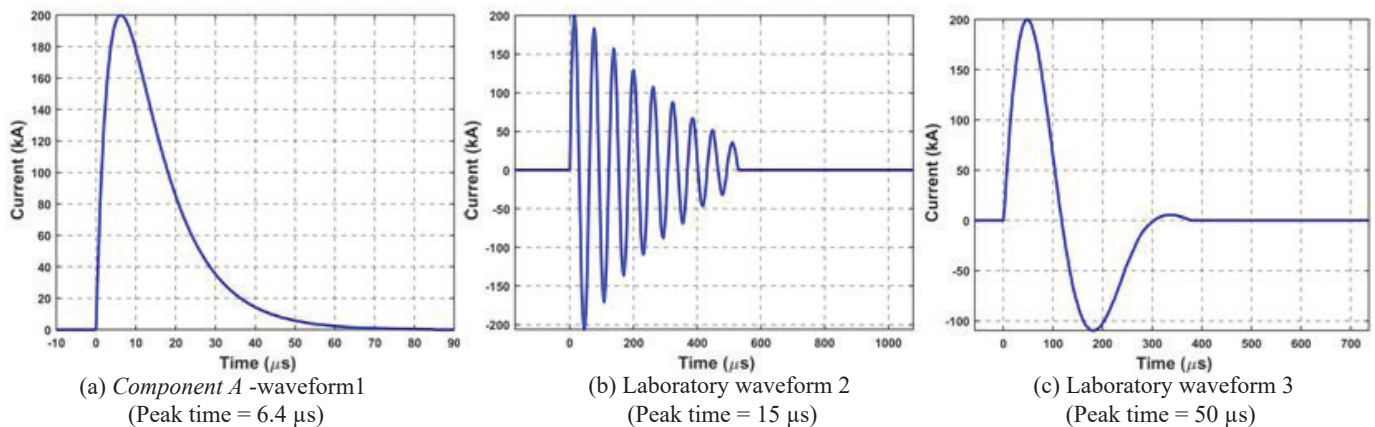


Fig. 4. Injected current waveforms

Current Waveforms

Three waveforms with different rise times are employed for the present work. First is the current *component A* (here referred to as WF1), which is specified in SAE standards. Its peak time is about 6.4 μs and is representative of a worst-case scenario. The

other two waveforms are generated in different high-voltage laboratories in India. These are designated as waveform 2 (WF2) and waveform 3 (WF3). Waveform 2 and waveform 3 have a peak time of 15 μs and 50 μs , respectively. The magnitude of all three waveforms is taken as 200 kA for the ease of comparison of field quantities. Fig. 4 shows the three waveforms. Waveform 2 and waveform 3 are damped oscillatory in nature due to the presence of stray capacitance in practical current generators.

Results and Discussion

As pointed out earlier, lightning attachment to the aircraft occurs at the extremities, which are also the injection and ejection points. Consequently, reference [10] has defined the list of injection and ejection points to be taken while performing LCI tests. For analysis, in the present paper current injection point is taken at the nose cone tip (i.e. X) and ejection is taken at the tail side (i.e. Y) as in Fig. 1. However, for the case which includes the RC, ejection is taken at the fore end of the aircraft (Fig. 2). By using the numerical methodology stated in section III, current and potential distribution on aircraft with and without RC for three different peak times of currents are obtained. Surface current density is plotted for all these cases for 200 kA current and at their corresponding peak times. A comparison of surface current density distribution with and without RC is made. The distribution obtained when the aircraft is injected with *component A* and without RC represents the actual/worst-case scenario. The distribution with RC represents a laboratory environment.

Case I: Waveform 1 is injected

Among the three waveforms, waveform 1 has the fastest peak time (6.4 μs), with an upper bound frequency of about 100 kHz [12]. At this frequency, eddy currents would dominate the current distribution [12]. The central fuselage of the aircraft is cylindrical in shape; hence, the current distribution is uniform in the fuselage. However, the wings of the aircraft are similar to thin plates, and eddy currents would lead to an increase in current density at wing edges and the current density will gradually reduce to a low value in the central region of the wing. The current density is found to fall rapidly from these wing edges. To capture this variation, a very fine discretisation is employed.

The surface current density distribution on aircraft without RC for WF1 (for 200 kA injected current) is shown in Fig. 5. From the plot, it can be observed that the maximum current density on aircraft is about 430 kA/m, which occurs at the injected/ejection points. However, this high current density has masked the current density variation in other regions as they have comparatively low current densities. Hence, for better visualisation of field quantities, the current distribution on the wing is extracted and shown with the aid of an arrow (Fig. 5). The high current density (113 kA/m) is confined to a very narrow region at the wing edges/tips. Away from the edges, current density falls to a value of less than 10 kA/m.

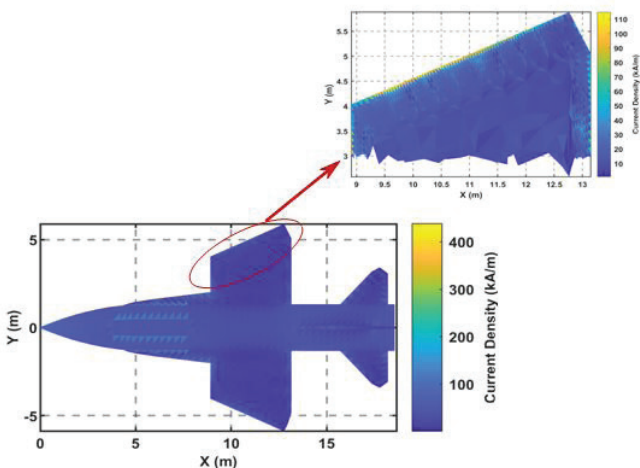


Fig. 5. Current density distribution (surface) without RC at peak instant i.e. 6.4 μs (for WF1)

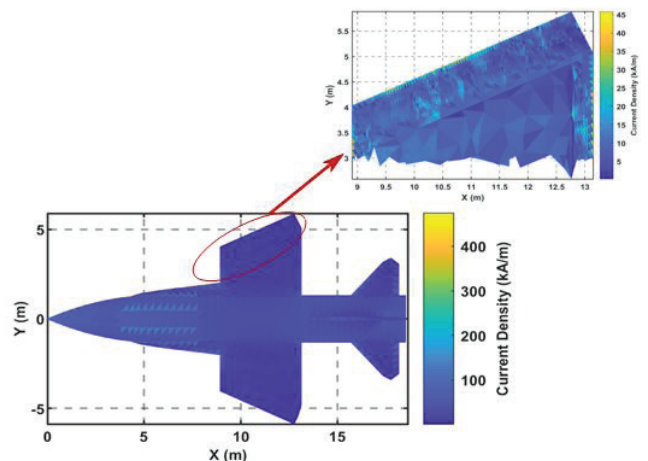


Fig. 6. Current density distribution (surface) with RC at peak instant i.e. 6.4 μs (for WF1)

Similarly, the plots for the current density distribution on aircraft for the case, which includes the RC are shown in Fig. 6. The maximum current density of aircraft is about 470 kA/m. It can be observed that there is a significant difference in the current

density at the wing edges as compared to that of the case without RC. Firstly, the maximum current density on the wing has reduced from 113 kA/m to 46 kA/m. Secondly, the presence of RC has made current distribution more uniform i.e., the rate of decay of the current density from the edges is very slow.

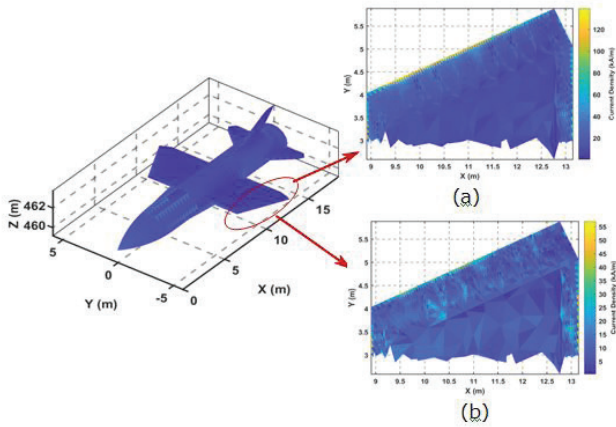


Fig. 7. Current density distribution (surface) at peak instant i.e. 15 μs (for WF2) (a) Without RC (b) With RC

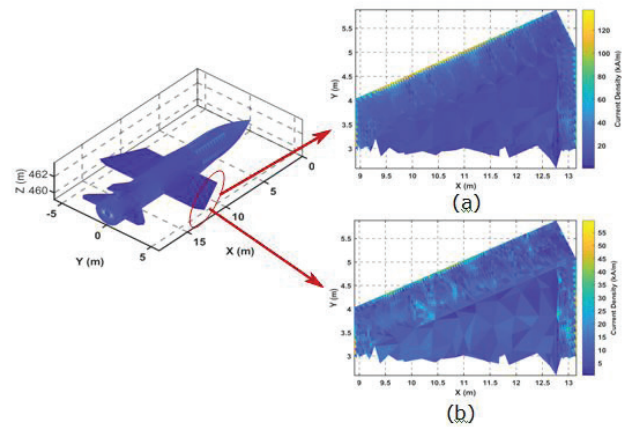


Fig. 8. Current density distribution (surface) at peak instant i.e. 50 μs (for WF3) (a) Without RC (b) With RC

Case II: Waveform 2 is injected

As mentioned earlier, waveform 2, shown in Fig. 4(b), is generated in the laboratory to carry out LCI tests. This waveform has a peak time that is about two to three times that of the standard current component A. Simulation results on aircraft due to this waveform with and without RC can be found in Fig. 7(a) and Fig. 7(b), respectively. It is inferred once again that the eddy currents have resulted in the concentration of current density at the edges, as in Fig 7(a). However, with RC, this distribution has become more uniform, as in Fig. 7(b). The actual current density on the wing (without RC) is about 128 kA/m, which is reduced to about 56 kA/m in the presence of RC. Also, it can be observed that as compared to waveform 1, the current density w.r.t waveform 2 is increased by about 13%.

Case III: Waveform 3 is injected

The current distribution on aircraft with and without the RC for waveform 3 (peak time 50 μs) can be found in Fig. 8. Once again, it is found that the current density on wings without RC is higher than that with RC.

Table 1. Maximum current density on wing

	Without RC (kA/m)	With RC (kA/m)	%Decrease
WF1 (6.4 μs)	113	46	59
WF2 (15 μs)	128	56	56
WF3 (50 μs)	127	58	54

It can be observed that in all the cases, wing current density plots without RC all look alike; however, the maximum value is different in different cases. Table I summarises the maximum current density obtained in all the cases with and without RC for 200 kA injected current evaluated at their corresponding peak times. From Table I, it can be inferred that the current density on the wing is high without RC; however, with RC, there is a reduction in current density of about 50% to 60% (for all waveforms). It clearly indicates the influence of RC on current distribution. Also, the current density is low for WF1 and increases to about 13% for WF2 and WF3. The dependency of surface current distribution on the rise time of current, as well as the RC arrangement, is studied. Based on the analysis done, it is concluded that the surface current distribution emulated in a laboratory test is quite different from that encountered by an aircraft in an actual lightning strike.

Conclusions

Lightning protection systems form an integral part of any aircraft design. Standards have devised current injection tests to measure the efficacy of these systems. Based on in-flight measurements, standard current waveforms are developed for these tests. However, it is rather difficult to build generators that produce such a current waveform (magnitude 200 kA and peak time 6.4 μ s). Also, the loop inductance increases the rise time of the waveform. Therefore, the laboratory waveforms are much slower than the actual waveforms. Due to this, the surface current distribution on aircraft reproduced in laboratory tests is not the same as the in-flight distribution. The field due to return conductors would also influence the current and field distribution on aircraft. The deviation in current distribution is much more prominent in the wing regions than in the central fuselage region. By means of simulation exercises on SDM aircraft, current distribution with and without RC is evaluated using the impedance network method. The distribution is also obtained with three waveforms having different peak times: the standard *component A* and two different laboratory waveforms. It is found that with RC, the current distribution on the wing has been reduced to about 50-60% as compared to that without RC. Also, it is found that the rise time of the current waveform has altered the distribution. The limitations of the laboratory tests in reproducing the actual current distribution should be considered while designing protective systems for aircraft.

References

1. F. Fisher, J. A. Plumer, and R. A. Perala, "Aircraft Lightning Protection Handbook," Lightning Technologies Inc Pittsfield MA, Tech. Rep., 1989.
2. A. I. B. Norway, "Report on the aircraft accident at Bodo airport on 4th December 2003 involving Dornier DO 228-202 LN-HTA, operated by Kato Airlines," Accident Investigation Board Norway, Tech. Rep., 2007.
3. I. A. C. A. A. I. Commission, "Interim report on accident investigation of Aeroflot Sukhoi Superjet 100 (RRJ-95B) aircraft in 2019," Interstate Aviation Committee Air Accident Investigation Commission, Tech. Rep., 2019.
4. M. Uman and V. Rakov, "The interaction of lightning with airborne vehicles," *Progress in Aerospace Sciences*, vol. 39, no. 1, pp. 61–81, 2003.
5. B. Fisher and J. Plumer, "Lightning attachment patterns and flight conditions experienced by the NASA F-106B airplane from 1980 to 1983," in *22nd Aerospace Sciences Meeting*, 1984, p. 466.
6. P. Laroche, M. Dill, J. Gayet, and M. Friedlander, "In-flight thunderstorm environmental measurements during the landes 84 campaign," *ONERA, TP*, no. 1985, p. 9, 1985.
7. H. D. Burket, L. C. Walko, J. S. Reazer, and A. V. Serrano, "In-flight Lightning Characterization Program on a CV-580 aircraft," Air Force Wright Aeronautical Labs Wright-Patterson Afb Oh Flight Dynamics Lab, Tech. Rep., 1988.
8. M. Buguet, P. Lalande, P. Laroche, P. Blanchet, A. Bouchard, and A. Chazottes, "Thundercloud electrostatic field measurements during the inflight EXAEDRE campaign and during lightning strike to the aircraft," *Atmosphere*, vol. 12, no. 12, p. 1645, 2021.
9. ARP-SAE, "5412: 2013," *Aircraft Lightning Environment and Related Test Waveforms. SAE Aerospace. USA*, pp. 1–56, 2013.
10. ARP-SAE, "5416: 2013," *Aircraft Lightning Test Methods. SAE Aerospace. USA*, pp. 1–145, 2013.
11. Surekha Jonnalagadda and Udaya Kumar, "Some observations pertaining to the adequacy of lightning current injection tests to aircraft," in *12th Asia-Pacific International Conference on Lightning (APL)*. IEEE, 2023, pp. 1–5.
12. Surekha Jonnalagadda, Udaya Kumar, "Identification of Suitable Governing Equation for Electromagnetic Fields in Aircrafts During a Lightning Strike," in *36th International Conference on Lightning Protection (ICLP)*, 2022, pp. 116–121.
13. R.-T. Huang, Y.-T. Duan, L.-H. Shi, Q. Zhang, L.-Y. Su, and S. Qiu, "Direct Current Injection Test Devices on Metal Cylinder: Experiment and Numerical Simulation," *IEEE Access*, vol. 7, pp. 65870–65876, 2019.
14. R. Huang, Y. Duan, K. Luo, and L. Shi, "Simulation research on the return conductor configuration for lightning indirect effect test of metal cylinder," in *IEEE 5th International Symposium on Electromagnetic Compatibility (EMC-Beijing)*, 2017, pp. 1–4.
15. L. P. Erm, "An experimental investigation into the feasibility of measuring static and dynamic aerodynamic derivatives in the DSTO water tunnel," Defence Science and Technology Organisation Fishermans Bend (Australia), Tech. Rep., 2013.
16. F. Terman, "Radio engineers' handbook (New York, 1943)".